

An Aspect of Hall-Petch Effect in Metallograin Structure

Michihiko Nakagaki¹, Shuji Takashima², Ryosuke Matsumoto¹, and Noriyuki Miyazaki²

Abstract: The present paper focuses on the micromechanical phenomena occurring in the polycrystalline metal materials. Correlations between the material hardening and the plastic lattice dislocation were discussed with the presence of the grain boundary. The characteristic distribution of the plastic strain gradient is numerically recognized, and hence the validity of incorporating the strain gradient term in the constitutive law is demonstrated. Also, the modeling of the inclusion interface sliding and debonding was performed on the equivalent inclusion theory to develop the constitutive law for the composite. The sliding model is considered to be effective to model the superplastic behavior of highly ductile metals. The superplastic phenomenon was recognized in the numerical test with the use of the presently suggested particle dispersed model, and its mechanism was attempted to be explained.

keyword: Polycrystal, Hall-Petch effect, Strain gradient, Size effect, Super plasticity, Grain sliding, Equivalent inclusion model, Self-consistency

1 Introduction

Development of advanced metal materials with the high level performance of strength has been the engineering aim in the technological history. As shown by Matsumoto et al. (2005), and by Nakamura et al. (2005), crystal grain structure in the metal has much to do with material's strength as well as its characteristic performance with respect to its ductility.

The continuum theory based solely on strain hardening with no strain gradient dependence would find no size effects. As it will be easily understood, finite element analyses of structures of different sizes but proportional where an elastoplastic material constitutive law is assumed with no strain gradient effects will return the same stress and strain results. However when the size is very small, it has generally been well known that the size does

matter on the behavior of the material performance. Plastic behavior of metal in the metal matrix composites is significantly affected by the inclusion size. Tomita et al. (2000) have investigated the mechanical characteristics of the particle reinforced metal-matrix composites by a finite element analysis with embedded strain gradient effects, and found the effects of the volume fraction, size and distribution pattern of the reinforcement particles on the macroscopic mechanical property of the composite. It was predicted that the flow stress is proportional to the inverse of the particle spacing. The effect has been known as Hall-Petch effect, which states that the yield strength of pure metals increase with diminishing grain size. It is considered that the enhancement of the metal is associated with the pile up of dislocations occurring in the vicinity of the grain boundary area inside the crystal grains. Propagation of the dislocations is prohibited through the grain boundary, as a consequence elevating resistance of the shear force that causes the dislocations. As the grain size is smaller, the total surface area of the grain boundary is greater, thus the flow strength becomes higher than those with the larger grain size.

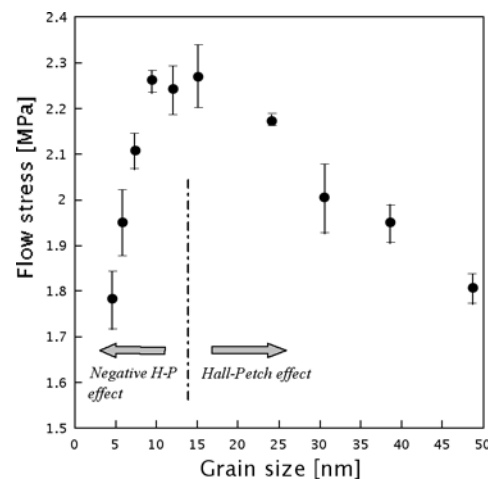


Figure 1 : Hall-Petch effect on flow stress (Schjøtz and Jacobsen (2003)).

Publicized evidence by Schjøtz and Jacobsen (2003) for

¹ Kyushu Institute of Technology, Fukuoka, Japan

² Kyoto University, Kyoto, Japan

copper in Figure 1 shows the apparent rise of the flow stress as the grain size becomes smaller. But when the grain size is even smaller than 10 to 15nm, the strength falls from the peak, which is known as “Negative Hall-Petch” effect. In this grain size range, it is thought that slipping on the grain surface with the neighboring grains plays a significant role rather than the ingrain crystal dislocations, and it would overwhelm the effect from the ingrain dislocation resistance. Schiøtz and Jacobsen (2003), Swaygenhoven et al. (2001), and others have extensively studied the nano-mechanism occurring at the crystal level by using molecular dynamics method, and its molecule level dislocation mechanism relevant to Hall-Petch effect is becoming unveiled.

For some metals, this phenomenon would occur even at greater grain sizes of one hundred times or even more the peak strength size. This effect is generally known as super plasticity. At high temperatures, some materials with certain microstructure exhibit high elongation strain ranging from several hundreds to one thousand percent when deformed under a tensile loading condition. Superplastic aluminum alloys generally have fine grain structure of about $10\mu\text{m}$ in diameter, where the grain size is controlled by adding some elements that suppress the grain growth. Since the grain boundary sliding during deformation becomes activated under these conditions, those alloys exhibit an extremely large degree of ductility. In an industrial application such as in forging, development of the most suitable material becomes increasingly important, and thus the through understanding of the phenomena of the superplasticity is required.

The effects of strain gradient in relevance to the material performance increasingly draw attention, and its significance of analysis on the subject has been emphasized by Tang, Shen, and Atluri (2003). The objective of the present paper is to identify that the micro mechanical strain gradient is responsible for the flow strength of plastic materials and to verify that the material strength is dependent on the grain size through the plastic strain gradient. Also presented in this work is the investigation of the superplastic phenomena closely related to the grain surface sliding. The work includes a development of a grain sliding model and a finite element analysis of grain dispersed composite employing the constitutive law accounting for the strain gradient effect suggested by Zbib (1994). Also included is an analysis of a polycrystalline material domain under tension, where the crystal slip

model in the work of Needleman et al. (1985) is used to describe the constitutive law for each crystal with different slide orientations.

2 Grain Size Depended Hardening: Strain Gradient

In the following sub-sections, the strain gradient effects due to the inclusion particle size on the strength of the composite of the ductile matrix material are examined. The constitutive law uses hypothetical hardening model including the harmonic plastic strain gradient term suggested by Zbib (1994). However, the validity of the model assuming the strain gradient has not yet been checked. Hence the present effort also includes some attempts to address the same subject in an utterly different approach independent of the above-mentioned constitutive model, trying to find the phenomenon of the plastic strain pile-ups, relevant to the material hardening, on the boundary area of the crystal grains.

2.1 Strain gradient dependent hardening model

Zbib modified the conventional yield condition in order to circumvent the difficulty encountered in dealing with the post-localization problem so that the gradient dependent flow stress is defined,

$$\boldsymbol{\tau} = \boldsymbol{\kappa}(\boldsymbol{\gamma}) - g \quad (1)$$

where, the gradient strain terms are given as in the following, generally including higher order terms of the effective plastic strain g such that,

$$g = c_1 \nabla^2 \boldsymbol{\gamma} + c_2 \nabla \boldsymbol{\gamma} \cdot \nabla \boldsymbol{\gamma} + c_3 \nabla^4 \boldsymbol{\gamma} \dots \quad (2)$$

Thus, it leads to allowing to include the length scale into the plastic constitutive law for composites with inclusions. Such is the case usually seen in a metal matrix composite where the matrix undergoes varied plastic deformations in the micro structure domain due to interactions between particles. If the material isotropy should be retained, the odd order terms must be deleted in the above. In the present, only the first term is retained for simplicity.

$$\boldsymbol{\tau} = \boldsymbol{\kappa}(\boldsymbol{\gamma}) - c_1 \nabla^2 \boldsymbol{\gamma} \quad (3)$$

In this paper, this plastic flow rule is used to analyze the inclusion size effect of a particle dispersed composite domain. Three types of the composite domain patterns are

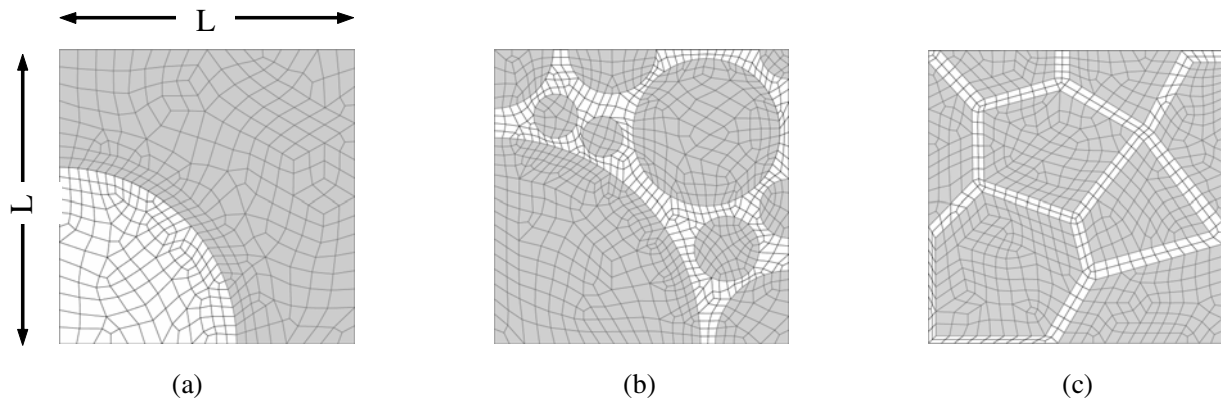


Figure 2 : Composite domains for FEM analyses with various grain sizes.

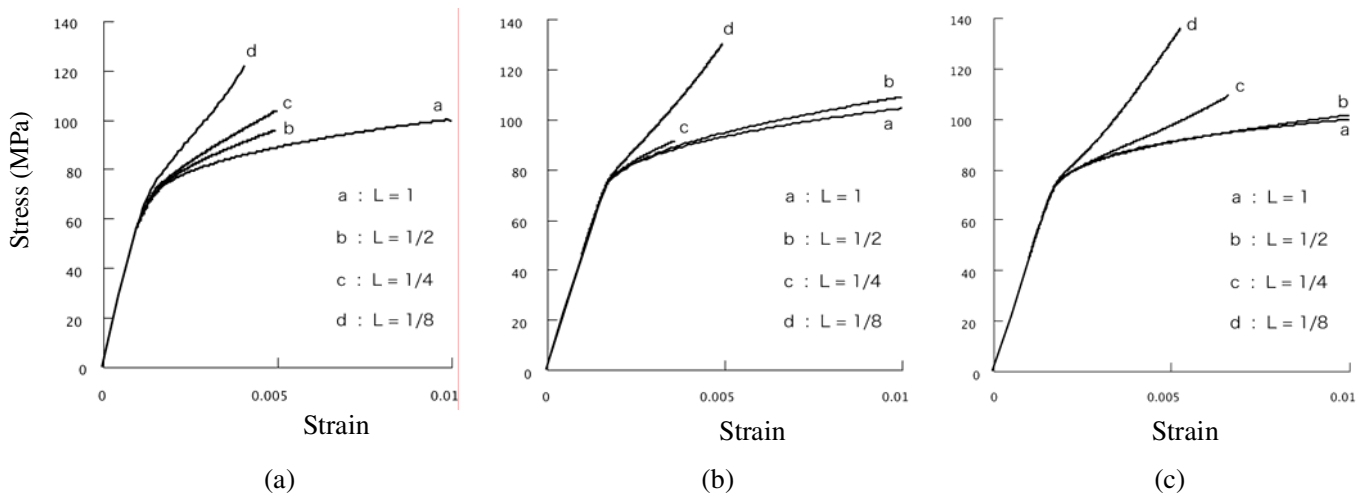


Figure 3 : Effect of plastic strain gradient over size scale.

considered and depicted in Figure 2 (a), (b), and (c). A finite element analysis is used for a unit domain with the mirror symmetric type boundary conditions representing the infinite composite domain subjected to a remote tensile loading. In those three models, the left vertical edges were constrained in lateral direction, the bottom edges in vertical direction, and the lateral displacements of the right edge and the vertical displacements of the top were enforced to be homogeneous by way of imposing penalties on the respective nodal displacements. To estimate the strain gradient term at an arbitrary integration point in the plastic domain, an influence area, which is circular, is set around the point. On all the data points within the area, the least square fitting was performed with the complete quadratic function to calculate the plastic strain gradient.

In Figure 2(a), the inclusion is the case, regularly arranged circular inclusions of 28% volume fraction in the plastic medium. The inclusions remain elastic being relatively harder than the matrix. Figure 2(b) is the case the volume fraction of the inclusion is 80% of the entire domain, but in this case the inclusions take the role of the plastic domain. The random distribution of the particles is supposed to provide a rather macro-isotropic nature of the composite.

Figure 2(c) is for the case representing a poly-crystal body with thick grain boundaries.

For the three cases of the composite models mentioned above, the inclusion size was varied by changing the representative scale length, L , in these figures. If the strain gradient term in the constitutive law were not accounted for, the macro stress-strain behaviors for the three mod-

els should respectively be the same even for the different scale factors.

Calculated global stress-strain results with the strain gradient assumption in the constitutive law are shown in Figure 3 (a), (b), and (c) for the respective analysis domain models in Figure 2. Calculated for all the four cases of the scale length $L=1, 1/2, 1/4,$ and $1/8$, the results show an evident propensity of hardening on the global strength curves as the inclusion size are varied. Relative to the standard size, $L=1$, results of all the smaller particle sizes have shown higher stress levels. Irrespective of the plastic strain gradient's evolution in matrix or inclusion, or of the microscopic geometry, enhancement of the material strength is acknowledged as the inclusion size becomes finer even with the same volume fraction of the particle dispersed composite.

2.2 Crystallograin analysis

The effect of the strain gradient is, thus, demonstrated, in the above, for composite materials by incorporating the gradient term in the strain hardening model for the plastic domain, and it successfully formulates the dependence of the particle size. In this subsection, another approach is tried in an attempt to obtain the same effect for the same phenomenon but without using the strain gradient terms assumed a priori.

Consider a strip of a polycrystalline metal material domain that consists of a number of crystal grains as depicted in Figure 4 for three different average grain sizes. As a whole, the global domain is supposed to be isotropic, but each grain is set to have different and random crystal lattice orientations. Under a severe loading, crystals will plastically deform in slip mode in accordance with the individual crystalline slip systems. In an expectation that the extension of the plastic slip arising from crystallographic dislocation due to shearing might be blocked by the grain boundary, a finite element analysis of the crystal domain was undertaken to investigate the plastic deformation mechanism in the grain. In order to properly treat the present problem, the crystal slip model originally suggested by Needleman et al. (1985) is used to describe the constitutive law for the finite element algorithm used herein.

Plastic deformation is considered to occur by shearing on the slip systems which consist of multiple slip planes. Using the expression of the power law form for the shear rates, the reference shear stress and strain relation for

each slip system α may be stated in the sum of other slips β as,

$$\dot{\boldsymbol{\tau}}^{(\alpha)} = \sum_{\beta=1}^n h_{\alpha\beta} \dot{\boldsymbol{\gamma}}^{(\beta)} \quad (4)$$

The description of the details can be found in the works of Needleman et al. (1985) and related materials. The constitutive law for single crystal relating the Jaumann rate of Kirchhoff stress and the stretch tensor can be stated by,

$$\dot{\boldsymbol{\tau}}_J = \mathbf{C} : \mathbf{D} \quad (5)$$

$$\mathbf{C} = \mathbf{L} - \sum_{\alpha} \sum_{\beta} (\mathbf{P}^{(\alpha)} : \mathbf{L} + \boldsymbol{\beta}^{(\alpha)}) \mathbf{N}_{\alpha\beta}^{-1} (\mathbf{P}^{(\beta)} : \mathbf{L} + \boldsymbol{\beta}^{(\beta)}) \quad (6)$$

where, \mathbf{L} is the elastic material tensor, and $\mathbf{P}^{(\alpha)}$ and $\boldsymbol{\beta}^{(\alpha)}$ are related to the current stress states and the deformation status.

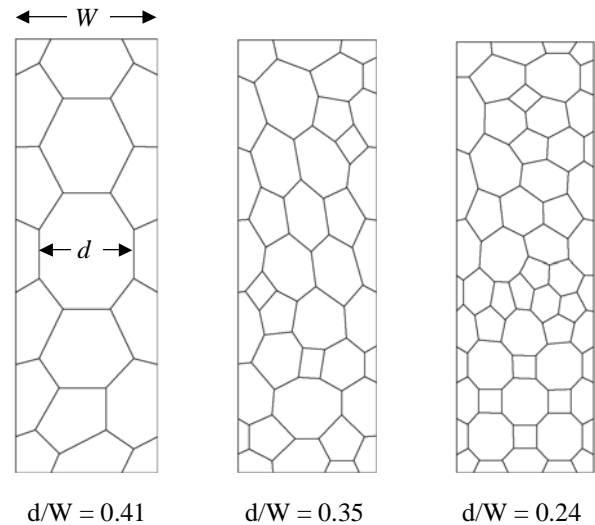


Figure 4 : Polycrystalline domains of tensile strip with various grain sizes.

For a plastic material of a power law hardening type, the three domains shown in Figure 4 were subjected to a longitudinal tensile loading in the present FEM analysis. As we know, in the finite element analysis and with the constitutive law as in the present, no size units are defined a priori or in the analysis procedure, whereas for the problems in Section 2.1, the incorporated strain gradient term in the constitutive law brings in the size dependence. Authors' intention in this section is to draw out the physical

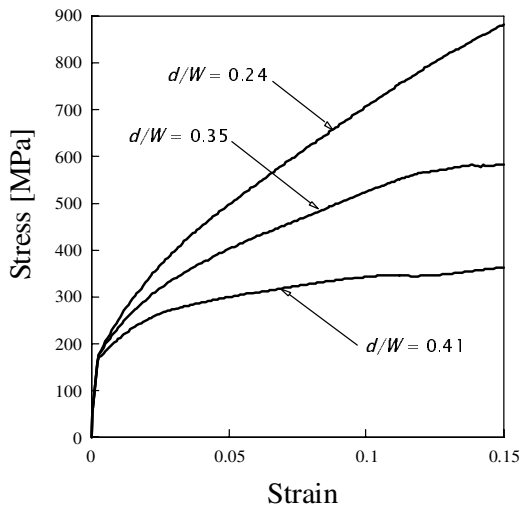


Figure 5 : Effect of grain size on stress-strain behavior.

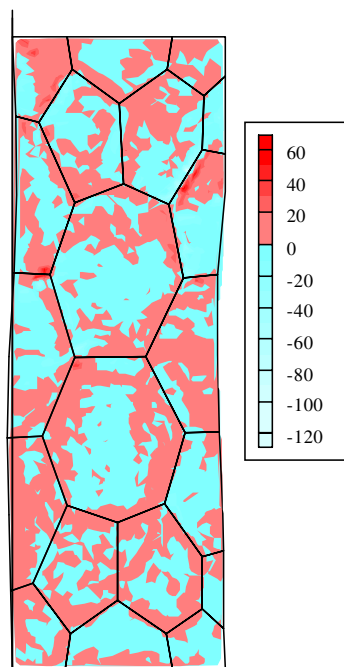


Figure 6 : (Color online) Distributed plastic strain gradient over polycrystalline domain in deformation.

phenomenon that the crystal size does matter in the deformation behavior of the metallograin structure, only from the crystal dislocation mechanism without assuming any hypothesis for strain gradient in the constitutive law a priori. One of the effective ways to define the size of the crystal grains is to define it made relative to some representative size of the problem, for which the strip width is selected.

The average grain size is varied in comparison with a representative scale size, which is the specimen width, W , such that, $d/W = 0.24, 0.35,$ and $0.41,$ respectively. Each crystal grain is subdivided with a number of triangular elements. The calculated global stress-strain behavior is shown in Figure 5 for the three cases of grain size. The present results that are not based on the hypothetical use of the plastic strain gradient term in the constitutive law also clearly show the dependence of the grain size on the global stress-strain behavior. In comparison with the result for $d/W = 0.41,$ the smaller grain size results obtain higher stress levels after the material is initially yielded. The trend of these results is similar to those obtained in Figures 3. The cause of the elevation of the strength is in the evolution of a resistance force to prevent the propagation of the plastic slip across grain boundaries. To view some signs of the phenomenon, distribution of the calculated plastic strain gradient, $\nabla^2\gamma,$ is plotted in Figure 6 for the coarse grain specimen case. The shaded or red areas denote the regions with the positive plastic strain gradient, or in other words, the region where the plastic strain is suppressed. The distribution appears biased toward the grain boundary. In the present analysis, no inter-grain substructure or materials are assumed, but only the orientations of the lattice are different across the boundary. Transmittance of the plastic slipping through the boundary is hindered when the dislocation propagates to dissimilar slip systems, thus raising the resistance to the local deformation as well as to the global. If the lattice orientation is the same all over the specimen domain, it is nothing more than a single crystal, and no distribution of the strain gradient will be observed then.

The similar phenomenon must be seen also in the other finer grain domain cases. Since the size dimension is smaller for the finer grains, the second derivative of the plastic strain is much greater and thus generates higher stress levels. Hence including the plastic strain gradient term in the strain hardening of the constitutive law is reasonable and effective for the class of problem where the plastic strain gradient takes effect, such as when Hall-Petch effect is significant. In industrial technology, this effect has already been utilized in metallurgical area to refine the crystal grain size and thus to enhance the ultimate strength of metal materials by adding some substances in the process of metal solidification. More recently, some mechanical process of effectively refining the crystal grain size to the order of nano size has been

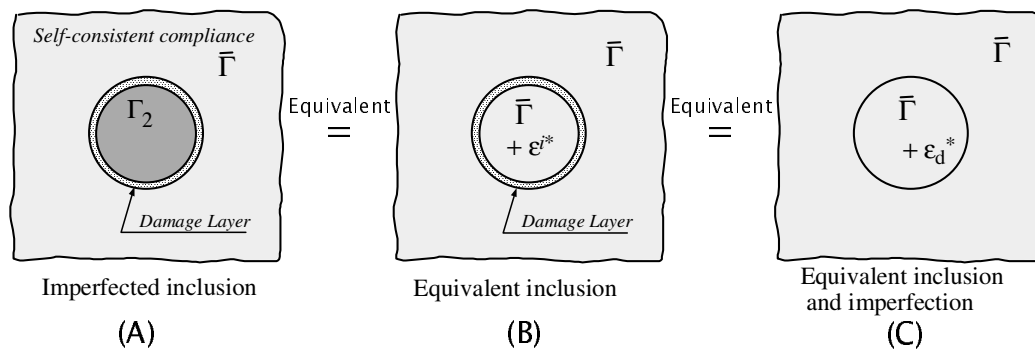


Figure 7 : Composite with imperfect interface and its equivalent domain.

successfully devised by applying a severe shear to the material, observing sixty percent increase of the flow stress on the tension test of a steel and aluminum alloys as well.

3 Grain Sliding Effects on Superplasticity

As discussed in the previous section, the enhancement of the plastic material is due to the resistance arouse when the propagation of the plastic slip is blocked at the grain boundary. Thus elevated ingrain stress might act upon the grain boundary, and especially when the size of the grain is even smaller, slipping might occur on the grain surfaces with each other. This is what it is considered to be the nano-mechanism for causing the negative Hall-Petch effect. As mentioned in the beginning in the introduction, the similar phenomenon occurring at even greater grain size is believed to be the superplasticity, which provides high ductility. Brass, which is the material suited for forging, consists of two phases of material, which are the coarse and hard α phase and the finer and relatively softer β phase. During the deformation process, sliding on the surface of the α phase grain is conspicuous accompanied by the extensive deformation of the β phase, while α phase grains themselves are hardly deformed. Polycrystalline metals material of single phase with the superplastic nature exhibit more like rearrangement of the grains as the results of an active surface sliding movement, rather than ingrain deformations. In the present effort, in coping with the micromechanical grain sliding problem, a particle dispersed composite modeling with sliding on the inclusion surface is performed.

3.1 Composite model with particle sliding

The basis of the present model is the self-consistent type equivalent inclusion theory, on which the constitutive model for a composite with the matrix of which undergoes elastoplastic deformations has been developed by Nakagaki and Wu (1999). In the present effort, consider a macroscopically homogeneous composite material with randomly dispersed particles. To develop a macro-constitutive model for the composite when particles undergo interfacial weakening, i.e., exfoliation and slide.

A two-fold equivalence modeling is devised. Depicted in Figure 7, consider a meso-domain in a composite, whose averaged macro-compliance, yet to be determined, is denoted by $\bar{\Gamma}$. The quantity with $(-)$ denotes the averaged value also to be determined according to the self-consistency. An inclusion particle is embedded in the averaged medium as shown in Figure 7(A), where a damage layer is modeled with a spring system between the inclusion and the surroundings. The model in (A) can be made equivalent to the model (B) in Figure 7, where the spring layer keeps unchanged but the properties of the core are replaced by those of the surrounding medium and an eigen strain, ϵ^{i*} , imposed to it. Further, the equivalent inclusion and the spring layer together are made equivalent to another virtual inclusion material with an eigen strain, ϵ_d^* , as shown in (C).

To model the particle interfacial imperfection, Gao (1995) used the spring layer model consisting of radial and tangential springs and obtained a particle solution of stresses and displacements using stress functions effective for all the spring compliance cases. He also gave a solution for the imperfect particle subjected to an eigen strain. With the use of these two solutions, the present

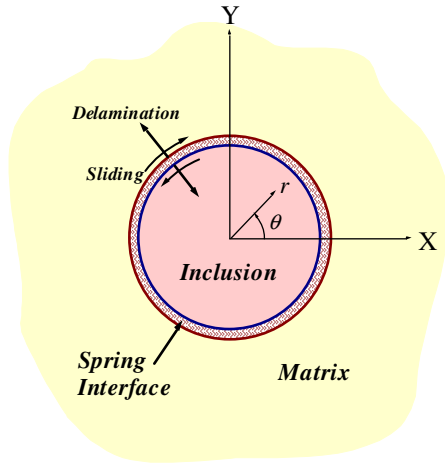


Figure 8 : Geometry of inclusion particle with spring layer.

equivalent inclusion model was developed. The radial and the tangential stresses on the interface of a disk inclusion are defined in relation to the displacement gaps Δu between the matrix (denoted by subscript 1) and the inclusions (subscript 2) across the interface that,

$$\sigma_{rr}(a, \theta) = \frac{n\mu_1}{a} \Delta u_r(a, \theta) \quad (7)$$

$$\sigma_{r\theta}(a, \theta) = \frac{k\mu_1}{a} \Delta u_\theta(a, \theta) \quad (8)$$

where a denotes a particle diameter, μ the shear modulus, and n and k are respectively the normal and tangential spring coefficients, as depicted in Figure 8. The condition, $k=0$ and $n = \infty$, represents the perfect sliding with no exfoliation, and $k = \infty$ and $n = \infty$ corresponds to the perfectly bonded interface. A damage strain tensor due to the interface imperfection can be expressed (Nakagaki et al. (2004)) in separable form with external load dependent terms and the eigen strain terms in the present equivalent process such that,

$$d\boldsymbol{\epsilon}^u = \mathbf{D}^\sigma : d\boldsymbol{\sigma}_0 + \mathbf{D}^* : d\boldsymbol{\epsilon}^{i*} \quad (9)$$

The damage tensor \mathbf{D}^σ is due to the external loading $\boldsymbol{\sigma}_0$; the nonzero components of the tensor will be described such that,

$$\begin{aligned} D_{1111}^\sigma &= D_{2222}^\sigma \\ &= \frac{\kappa_1 + 1}{2\mu_1} \left[\frac{1}{t\kappa_2 n - tn + 2n + 4} + \frac{(k+n)(1+t\kappa_2) + 12}{P} \right] \end{aligned}$$

$$\begin{aligned} D_{1122}^\sigma &= D_{2211}^\sigma = \frac{\kappa_1 + 1}{2\mu_1} \times \\ &\left[\frac{1}{t\kappa_2 n - tn + 2n + 4} - \frac{(k+n)(1+t\kappa_2) + 12}{P} \right] \end{aligned} \quad (11)$$

$$D_{1212}^\sigma = \frac{\kappa_1 + 1}{2\mu_1} \frac{(k+n)(1+t\kappa_2) + 12}{P} \quad (12)$$

While, the tensor \mathbf{D}^* represents the damage due to the assignment of the eigen strain $\boldsymbol{\epsilon}^{i*}$ to the equivalent core inclusion, and will be given by,

$$\begin{aligned} D_{1111}^* &= D_{2222}^* = -\frac{2}{t\kappa_2 n - tn + 2n + 4} \\ &- \frac{(k+n)(1+t\kappa_2) + 12}{P} \end{aligned} \quad (13)$$

$$\begin{aligned} D_{1122}^* &= D_{2211}^* = -\frac{2}{t\kappa_2 n - tn + 2n + 4} \\ &+ \frac{(k+n)(1+t\kappa_2) + 12}{P} \end{aligned} \quad (14)$$

$$D_{1212}^* = -\frac{(k+n)(1+t\kappa_2) + 12}{P} \quad (15)$$

In the above, t , κ , and P are the parameters compound of the spring coefficients and the composing phase materials, where the parameters used for the matrix material are made equivalent to its tangent moduli. Details of which will be found in the works of Nakagaki et al. (2004). In the matrix domain of plastic composite such as a metal matrix composite, the stress distribution is far from the uniform state but significantly varied caused by stress interaction between inclusions. Furthermore, the average stress-strain relation is significantly different from that of the homogeneous material, being influenced by the volume fraction of inclusions. In the works of Nakagaki et al. (1999), this important fact has been brought to attention in the constitutive law development. In this paper, the approach to account for the meso-local plastic effect in the matrix is utilized to develop the present particle-sliding model.

In order to account for the stress distribution in the matrix domain, it is natural to assume that the distribution is describable in Gaussian distribution function of the form,

$$P_1(\rho_1^i) = \frac{1}{\sqrt{2\pi}\phi} e^{-\frac{1}{2\phi^2}(\rho_1^i - 1)^2} \quad (16)$$

Suppose that thus distributed stress range in the matrix is (10) divided into a finite number of small stress segments. In a

segment, the stress increment tensor is related to the corresponding strain increment in the ordinary elastoplastic manner, but its degree of plastic yielding differs segment by segment. The variance, ϕ , that suffices the integral of P_1 by 99.7 percent of accuracy, can be determined with finite values of $\rho_1 s$ (plural form s) by,

$$\phi = \frac{\rho_1^{\max} - \rho_1^{\min}}{6} \quad (17)$$

where, ρ_1 is the equivalent stress normalized by the average value in the phase. In the present, the maximum and the minimum stresses in the matrix are determined from the closed form solutions around an elliptic inclusion given by Mura and Chen (1977).

In these process, the macro strain-stress relation of the elastoplastic composite with the modeled interfacial spring layer was derived in the final form of the composite constitutive law such that,

$$d\boldsymbol{\epsilon}_0 = \bar{\boldsymbol{\Gamma}} : d\boldsymbol{\sigma}_0 \quad (18)$$

$$\bar{\boldsymbol{\Gamma}} = \sum_{i=1}^n \Delta c_i \boldsymbol{\Gamma}_1^i : \mathbf{C}_0^i + \sum_{j=1}^m \Delta c_j \left[\begin{array}{l} \boldsymbol{\Gamma}_2^j : \left(\mathbf{I} + \bar{\mathbf{E}}_0 : \left[\left(\mathbf{I} + \mathbf{D}^* \right) : \bar{\mathbf{A}}_0^j + \mathbf{D}^\sigma \right] \right) \\ + \left(\mathbf{D}^\sigma + \mathbf{D}^* : \bar{\mathbf{A}}_0^j \right) \end{array} \right] \quad (19)$$

where, Δc_i is the volume fraction corresponding to the respective stress segment, tensor C_0^i describes the relation between the stress segment $d\boldsymbol{\sigma}_1^i$ and the external stress increment $d\boldsymbol{\sigma}_0$, is an updated value of a tensor related to the Eshelby tensor, and

$$\bar{\mathbf{A}}_0^j = \left[\left(\boldsymbol{\Gamma}_2^j - \bar{\boldsymbol{\Gamma}} \right)^{-1} - \bar{\mathbf{E}}_0 : \left(\mathbf{I} + \mathbf{D}^* \right) \right]^{-1} : \left(\mathbf{I} + \bar{\mathbf{E}}_0 : \mathbf{D}^\sigma \right) \quad (20)$$

The present composite material model for the particle interfacial imperfections was tested for its accuracy. A two-dimensional infinite domain of the composite under tension, in which the matrix is elastoplastic, whereas the inclusions stay elastic, was considered. The material domain was studied in two ways: first, by a finite element analysis of the composite with disc particles dispersed in the domain; another, by the presently developed constitutive model. The analysis of the finite element method

is performed on the model with normal and tangential springs around the particle on the interface for each inclusion.

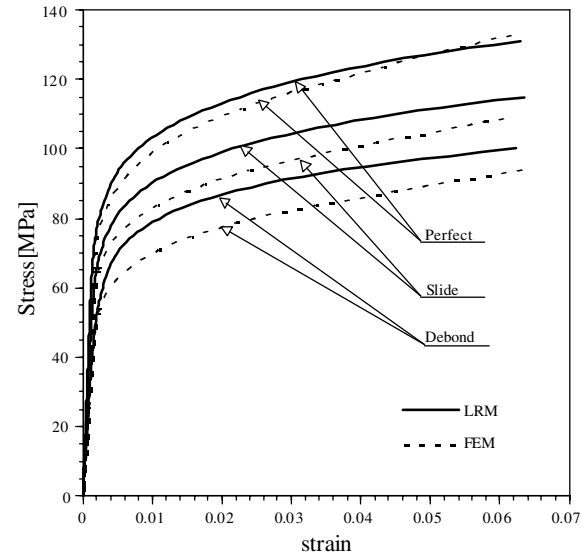


Figure 9 : Elastoplastic stress-strain results for the present model compared with the finite element analysis.

Calculated results of the global stress-strain relation for the volume fraction of 20 percent inclusions are shown in Figure 9 for three cases: i.e., the perfect interface; slide only; and debond only. The result of the present model for the intact interface case denoted by “Perfect” shows good correlations with the independent FEM results. Calculations of the present model on the slide only and the debond only have shown marginal results, however, exhibit very similar behaviors to those of the FEM in the plastic range.

The present constitutive model is embedded in the finite element system to analyze the effect of the grain interface sliding on the superplastic behavior. The modeled material is the particle dispersed composite strip of non-dimensional length, 3, and its aspect ratio is 3. The strip is elongated to 4 under a tensile load. The volume fraction of the composite is 10 percent, where both the matrix and the inclusions deform in elastic-plastic behavior, however the yield stress of these inclusions is relatively higher. Figure 10(a) shows the results of the case that both the matrix and the inclusions are of the same material, either of the matrix or the inclusion, and no sliding on the interface is allowed, i.e. $k = n = \text{infinity}$. Characteristic shear localization is seen in the center part of

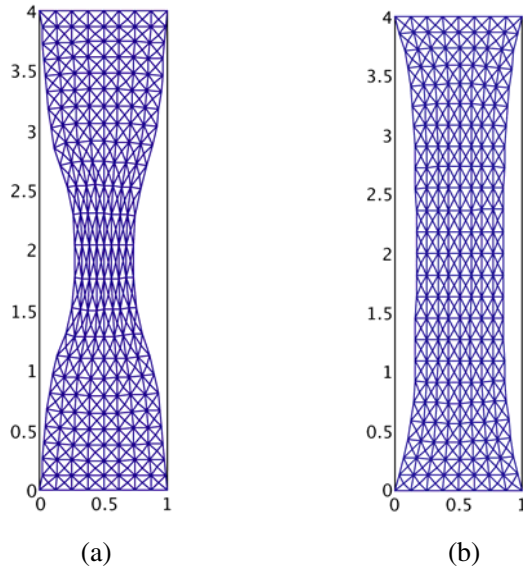


Figure 10 : Deformation types of elongated strip

the specimen. This is the typical deformation type of the monolithic isotropic metal materials. Figure 10(b) is the case that the yield strength of the inclusion phase is about twice that of the matrix, and the particle interface is allowed to slide, $k = 0, n = \text{infinity}$. The specimen uniformly deformed exhibiting no shear localization within the specimen. This is apparently due to the effects of the dispersed particles and the sliding on the surface. The deformation type of the latter is very much like that of the superplastic materials.

However, interesting is the fact that we have obtained during the course of the investigation of the present, that is even when the sliding is suppressed on the inclusion interface, the specimen elongates in the superplastic mode without necking if the volume fraction of the inclusion phase is sufficiently large such as more than several percent. Since the amount of the sliding on the particle surface is limited, it necessarily must jump to neighboring particles causing sliding there. The same can be true for the extensive plastic deformations occurring between the particles due to interaction. Thus, the micromechanical phenomena occurring in the material and causing the superplastic deformations maybe in the mechanism of dispersing the stress concentration among the particle dispersed geometry in the micrographic geometry of the material. The same principle can be applied to explain the superplastic effect in the polycrystalline metal materials.

4 Concluding remarks

Focusing on the micromechanical phenomena occurring in the polycrystalline metal materials or in the composite materials, correlations between the material hardening and the plastic lattice dislocation was made clear with the presence of the grain boundary. The characteristic distribution of the plastic strain gradient is numerically recognized, and hence the validity of incorporating the term in the constitutive law is demonstrated. Also in this paper, the modeling of interface-sliding and debonding of the inclusion were performed to develop the constitutive law for the composite. The sliding model is considered to be effective to model the superplastic behavior of highly ductile metals. The superplastic phenomenon was recognized with the use of the presently suggested particle dispersed model, and its mechanism was attempted to be explained.

References

- Gao, Z.** (1995): A circular inclusion with imperfect interface: Eshelby's tensor and related problems. *Journal of Applied Mechanics, Transactions of ASME*, Vol. 62, pp. 860-866.
- Matsumoto, R.; Nakagaki, M.; Nakatani, A.; Kitagawa, H.** (2005): Molecular-dynamics study on crack growth behavior relevant to crystal nucleation in amorphous metal. *CMES: Computer Modeling in Engineering & Sciences*, Vol. 9, No. 1, pp. 75-84.
- Mura, T. and Cheng, P. C.** (1977): The Elastic Field Outside an Ellipsoidal Inclusion. *Journal of Applied Mechanics, Transaction of ASME*, pp. 591-594.
- Nakagaki, M.; Matsumoto, R.; Nakamichi, Y.; Takashima, S.** (2004): Composite Material Model with Circular Inclusion under Imperfect Interface Conditions. *Proceedings of ICCES04*.
- Nakagaki, M. and Wu, Y. D.** (1999): Elastoplastic constitutive Model of Particle-dispersed Composite Accounting for Meso-Scopic Localization Effects. *Computer Modeling and Simulation in Engineering*, Vol.4, No.3 pp. 186-192.
- Nakamura, K.; Neishi, K.; Nakagaki, M.; Horita, Z.** (2005): Continuous grain refinement using severe torsion straining process. *Proceedings of 3rd International Conference on Nanomaterials by Severe Plastic Deformation*, pp. 385-390.

Needleman, A.; Asaro, R. J.; Lemonds, J.; Peirce, D. (1985): Finite element analysis of crystalline solids. *Computer methods in applied mechanics and engineering*, Vol. 52, pp. 689-708.

Schiøtz, Jakob and Jacobsen, Karsten W. (2003): A Maximum in the Strength of Nanocrystalline Copper. *Science* Vol. 301, No. 9, pp. 1357-1359.

Tang, Z.; Shen, S. and Atluri, S. N. (2003): Analysis of Materials with Strain-Gradient Effects: A Meshless Local Petrov-Galerkin(MLPG) Approach, with Nodal Displacements only. *CMES: Computer Modeling in Engineering & Sciences*, Vol. 4, No. 1, pp. 177-196.

Tomita, Y.; Higa, Y.; Fujimoto, T. (2000): Modeling and estimation of deformation behavior of particle-reinforced metal-matrix composite. *International Journal of Mechanical Sciences*, Vol. 42, No. 11, pp. 2249-2260.

Van Swaygenhoven, H.; Caro, A.; Farkas, D. (2001): A molecular dynamics study of polycrystalline fcc metals at the nanoscale: grain boundary structure and its influence on plastic deformation. *Materials Science and Engineering A*, Vol. 309, No. 310, pp. 440-444.

Zbib, H. M. (1994): Size effects and shear banding in viscoplasticity with kinematic hardening. *ASME AMD-Vol.183/MD-Vol.50, Material Instabilities: Theory and Applications*, pp. 19-33.